SLAC-PUB-14332

Longitudinal impedance due to coherent undulator radiation in a rectangular waveguide

G. Stupakov and D. Zhou

December 9, 2010

In this paper we investigate the longitudinal impedance due to coherent undulator radiation in a rectangular waveguide. We find that the impedance exhibits narrow peaks at resonant frequencies at which waveguide modes are in synchronism with particle motion in the undulator. Analytical calculations are compared with numerical simulations carried out with a computer code that solves parabolic equation for the electromagnetic field.

I. INTRODUCTION

Damping wigglers are used in several accelerator projects to decrease the emittance of a high-energy beam in the ring. Due to intensive radiation in the wiggler, it can generate an additional wakefield, similar to the coherent synchrotron radiation (CSR) wakefield in bending magnets, that contributes to the total impedance budget of the ring. In analogy with CSR, we call the wakefield generated due to the coherent wiggler radiation the CUR wakefield (with U standing for the "undulator"). Previously, the CUR wakefield was studied in Refs. [1–3] assuming radiation in free space. In this paper we calculate the impedance taking into account the vacuum chamber in the wiggler with conducting metallic walls.

CUR impedance inside a rectangular waveguide was also treated by Y.-H. Chin [4]. He developed a general method using field expansion into the waveguide eigenmodes. The focus of his work was the case of a weak undulator with a small undulator parameter $K \ll 1$. In this paper we will be interested in the opposite case of a large $K \gg 1$.

There are several simplifying assumptions that we use in our analysis. First, we assume that the amplitude of the wiggling motion of particles is much smaller than the transverse size of the vacuum chamber. Second, we consider a relativistic beam with the Lorentz factor $\gamma \gg 1$. As analysis shows, in the limit $K \gg 1$, all the radiation properties in such a wiggler depend only on the ratio K/γ which is equal to the maximal deflection angle θ_0 of the orbit relative to the axis of the wiggler. Introducing this parameter into the theory and replacing

Work supported in part by US Department of Energy contract DE-AC02-76SF00515.

SLAC National Accelerator Laboratory, Menlo Park, CA 94025

$K/\gamma = \theta_0$ we then can set $\gamma = \infty$. Hence, our particles are moving with the speed of light.

We will also assume that we are interested in calculation of the longitudinal impedance $Z(\omega)$ in a relatively low frequency range, $\omega \ll \omega_0$, where ω_0 is the frequency of the first harmonic of the wiggler radiation propagating along the axis. For a plane undulator and $K \gg 1$, this frequency is given by $\omega_0 = 4ck_w/\theta_0^2$, where $k_w = 2\pi/\lambda_w$ with λ_w the wiggler period. Hence we limit our consideration to

$$k \ll k_0, \tag{1}$$

where $k_0 = c\omega_0$. Note that, accorindg to [2], in this limit the CUR longitudinal impedance in free space is

$$Z(k) = \frac{1}{4} Z_0 L_w k \frac{k_w}{k_0} \left[1 - \frac{2i}{\pi} \left(\log \frac{4k}{k_0} + \gamma_E \right) \right], \tag{2}$$

where L_w is the wiggler length, $Z_0 = 377$ Ohm, and $\gamma_E = 0.577$ is the Euler constant. Eq. (2) is valid in the limit of large number of periods in the wiggler, $N_w = L_w k_w/2\pi \gg 1$.

Due to our assumption (1), it turns out that in addition to the approximation $v = c$ one can use even a stronger approximation $v_z = c$. Indeed, during the motion in the wiggler, the difference $\Delta v = c - v_z \sim c\theta_0^2$. It can be neglected if the phase accumulated due to this difference over one period of the wiggler between the electromagnetic wave propagating with the speed of light and the particle is much smaller than π, that is $k\lambda_w \Delta v/c \sim k\lambda_w \theta_0^2 \ll \pi$. The last inequality is equivalent to (1) if one takes into account that $k_0 = 4k_w/\theta_0^2$.

In this work we assume that the walls of the vacuum chamber have a perfect conductivity, and neglect resistive wall losses.

II. THE METHOD

We will calculate the real part of the longitudinal impedance $\mathrm{Re}\, Z$ using a relation [5] between $\mathrm{Re}\, Z$ and the spectral power of radiation $P(\omega)$ of a point charge q

$$\mathrm{Re}\, Z(\omega) = \frac{\pi}{q^2} P_\omega \,. \tag{3}$$

Although knowledge of only $\mathrm{Re}\, Z$ does not give a complete solution of the wakefield problem, it is useful for comparison and benchmarking computer codes. Moreover, as we will see in what follows, it indicates the existence of narrow high peaks in the impedance, which might contribute to the beam instability.

We will use the Fourier transformed fields and current, which means the time dependence of all involved quantities $\propto e^{-i\omega t}$. These quantities are marked with the subscript ω; the inverse Fourier transformation has a form

$$\frac{1}{2\pi}\int_{-\infty}^{\infty} \boldsymbol{E}_\omega e^{-i\omega t} d\omega, \tag{4}$$

with similar expressions for the magnetic field and the current density.

The radiation field of a particle in a waveguide can be computed using the general formalism of Vainshtein [6]. It is represented as a sum of waveguide eigenmodes of which we only leave the modes propagating in the forward directions $\boldsymbol{E}_n^+$ (the energy radiated into the modes in the opposite direction is negligible for a relativistic beam)

$$\boldsymbol{E}_\omega^{\mathrm{rad}} = \sum_n a_n \boldsymbol{E}_n^+, \tag{5}$$

where n denotes a collection of parameters that identify a mode. For a given n the mode can also propagate in the negative direction; the field of this mode is denoted by $\boldsymbol{E}_n^-$. The mode amplitudes a_n given by the following expressions

$$a_n = -\frac{1}{N_n}\int \boldsymbol{j}_\omega \cdot \boldsymbol{E}_n^- dV, \tag{6}$$

where $\boldsymbol{E}_n^-$ is the electric field of the mode propagating in the negative directions and the mode norm N_n is

$$N_n = \frac{c}{4\pi}\int \left(\boldsymbol{E}_n^+ \times \boldsymbol{H}_n^- - \boldsymbol{E}_n^- \times \boldsymbol{H}_n^+\right) \cdot d\boldsymbol{S}. \tag{7}$$

The integration in the last integral goes over the cross-section of the waveguide (the value of the integral does not depend on the position of this cross-section). Introducing the energy flow P_n in mode n as an integrated over the cross-section and averaged over time the Poynting vector,

$$P_n = \frac{c}{8\pi}\int \mathrm{Re}(\boldsymbol{E}_n^+ \times \boldsymbol{H}_n^{*+}) \cdot d\boldsymbol{S}, \tag{8}$$

it is easy to show that

$$P_\omega = \frac{2}{\pi}\sum_n P_n |a_n|^2. \tag{9}$$

Note also that for modes in rectangular waveguide $N_n = 4P_n$.

III. BEAM ORBIT AND CURRENT DENSITY

We assume that the particle trajectory lies in the $y = 0$ plane and is defined by the equations $x = x_0(t)$ and $z = z_0(t)$. Then the current density associated with the moving point charge is

$$\boldsymbol{j}(x, y, z, t) = \boldsymbol{v}(t) q \delta(x - x_0(t)) \delta(y) \delta(z - z_0(t)), \tag{10}$$

where $\boldsymbol{v}(t) = dx_0(t)/dt$ is the velocity. The Fourier transformation of the current is

$$\begin{aligned} \boldsymbol{j}_\omega(x, y, z) &= \int_{-\infty}^{\infty} dt e^{i\omega t} \boldsymbol{j}(x, y, z, t) \\ &= q \int_{-\infty}^{\infty} dt e^{i\omega t} \boldsymbol{v}(t) \delta(x - x_0(t)) \delta(y) \delta(z - z_0(t)). \end{aligned} \tag{11}$$

Changing the integration variable from t to z_0 (we assume that $z_0(t)$ is a monotonically increasing function of t) we obtain

$$\boldsymbol{j}_\omega(x, y, z) = \frac{q}{v_z(z)} e^{i\omega t(z)} \boldsymbol{v}(z) \delta(x - x_0(z)) \delta(y), \tag{12}$$

where the time is expressed through the z coordinate by inverting the function $z = z_0(t)$ and all the time-dependent variables are expressed as functions of z by substituting $t \to t(z)$.

Let us take for the orbit in the undulator

$$x_0(z) = x_a(1 - \cos k_w z), \tag{13}$$

where x_a is the amplitude of the oscillations. This choice of the functional dependence for x_0 is dictated by the fact that at the entrance to the wiggler, at $z = 0$, both the initial value of x_0 and the initial angle dx_0/dz are equal to zero. The maximal angle of the orbit dx_0/dz is θ_0,

$$\theta_0 = k_w x_a, \tag{14}$$

which, as was pointed out in the Introduction, we assume to be small, $\theta_0 \ll 1$.

If the particle velocity is v then the $t(z)$ dependence can be found from the equation

$$t = \frac{1}{v} s(z) = \frac{1}{v} \int_0^z dz' \left(1 + \frac{dx_0(z')}{dz'}\right)^{1/2}, \tag{15}$$

where $s(z)$ is the length of the orbit measured from the initial point $z = 0$. Using the smallness of θ_0 and keeping only terms of the second order in θ_0 one obtains

$$t = \frac{1}{v}\left(z + \frac{\theta_0^2}{4k_w}(k_w z - \frac{1}{2}\sin 2k_w z)\right). \tag{16}$$

As was discussed in the introduction, for our purposes, it is actually enough to use a simpler relation

$$t = \frac{z}{c} \tag{17}$$

corresponding to the motion with the speed of light in the z direction. Respectively, for $\boldsymbol{j}_\omega$ we then have

$$\boldsymbol{j}_\omega(x, y, z) = \frac{q}{c} e^{ikz} \boldsymbol{v}(z)\delta(x - x_0(z))\delta(y). \tag{18}$$

To separate the Coulomb field of the beam from the radiation, we will use the following approach. Consider an auxiliary point charge q moving along the axis z through the system with the speed of light: the orbit of this charge can be obtained by setting $x_a = 0$ in (13). Since the orbit of this charge is a straight line, it does not radiate, and its electromagnetic field consists of the moving Coulomb field only. Denote the difference between $\boldsymbol{j}_\omega$ and the current of the auxiliary charge by $\Delta\boldsymbol{j}_\omega$, and note that it is only nonzero in the wiggler region, being canceled at the preceding and following the wiggler straight parts of the particle orbit. Inside the wiggler, $0 < z < L_w$, $\Delta\boldsymbol{j}_\omega$ has two components $\Delta\boldsymbol{j}_\omega = (\Delta j_{\omega,x}, \Delta j_{\omega,z})$ with

$$\Delta j_{\omega,x} = \frac{q}{c} e^{ikz} v_x(z)\delta(x - x_0(z))\delta(y) = q x_0'(z) e^{ikz}\delta(x - x_0(z))\delta(y), \tag{19}$$

and

$$\Delta j_{\omega,z} = q e^{ikz}[\delta(x - x_0(z)) - \delta(x)]\delta(y). \tag{20}$$

IV. CALCULATION OF THE WAVE AMPLITUDES AND IMPEDANCE

We assume a rectangular waveguide of width a (in x direction) and height b (in y direction) with the origin of the coordinate system located at the center of the rectangle. We begin with calculation of the mode amplitudes of TM modes. In such a mode (of unit amplitude) propagating in the negative direction, the z-component of the electric field is given by

$$E_z^-(x, y) = \sin\left[k_x\left(x + \frac{a}{2}\right)\right]\sin\left[k_y\left(y + \frac{b}{2}\right)\right] e^{-ik_z z}, \tag{21}$$

where $k_x = \pi n_1/a$, $k_y = \pi n_2/b$, and $n_1 > 0$ and $n_2 > 0$ are positive integer numbers. In what follows, we will use $\varkappa = \sqrt{k_x^2 + k_y^2}$. The longitudinal component of the wavenumber in (21) is $k_z = \sqrt{k^2 - \varkappa^2} > 0$. The x component of the electric field in the mode is [7]

$$E_x^-(x,y) = -\frac{ik_z k_x}{\varkappa^2} \cos\left[k_x\left(x+\frac{a}{2}\right)\right] \sin\left[k_y\left(y+\frac{b}{2}\right)\right] e^{-ik_z z}, \tag{22}$$

and the averaged over time energy flow $P_{\rm TM}$ is

$$P_{\rm TM} = \frac{\omega k_z}{32\pi\varkappa^2} ab, \tag{23}$$

with $N_{\rm TM} = 4P_{\rm TM}$. Using notation $a_{\rm TM}$ for a_n of TM modes, from Eq. (6) and the currents (19) and (20) we obtain

$$\begin{aligned} a_{\rm TM} &= -\frac{1}{N_{\rm TM}} \int_0^{L_w} dz \int dxdy (\Delta j_{\omega,x} E_x^- + \Delta j_{\omega,z} E_z^-) \\ &= -\frac{q}{N_{\rm TM}} \int_0^{L_w} dz e^{ikz} \left(x_0'(z) E_x^-(0,0) + x_0(z) \left.\frac{\partial E_z^-}{\partial x}\right|_{x=0,y=0} \right). \end{aligned} \tag{24}$$

In the last integral we neglected x_0 in the argument of E_x^- and used the Taylor expansion for E_z^-. Using (13) for the orbit, it is not difficult to find

$$\begin{aligned} |a_{\rm TM}|^2 P_{\rm TM} = \frac{8\pi q^2 \theta_0^2 k_w^2}{\omega ab} \frac{k_x^2 \varkappa^2}{k_z} \left(\frac{k_z}{\varkappa^2} - \frac{1}{k-k_z}\right)^2 \frac{\sin^2[\pi N_u (k-k_z)/k_w]}{[(k-k_z)^2 - k_w^2]^2} \\ \times \cos^2\frac{\pi n_1}{2} \sin^2\frac{\pi n_2}{2}. \end{aligned} \tag{25}$$

In a TE mode of unit amplitude, the z-component of the magnetic field is given by

$$H_z^-(x,y) = \cos\left[k_x\left(x+\frac{a}{2}\right)\right] \cos\left[k_y\left(y+\frac{b}{2}\right)\right] e^{-ik_z z}, \tag{26}$$

where $k_x = \pi n_1/a$, $k_y = \pi n_2/b$, and one of the integers n_1 and n_2 can now be equal to zero. The x component of the electric field in the mode is [7]

$$E_x^-(x,y) = -\frac{ikk_y}{\varkappa^2} \cos\left[k_x\left(x+\frac{a}{2}\right)\right] \sin\left[k_y\left(y+\frac{b}{2}\right)\right] e^{-ik_z z}, \tag{27}$$

and the averaged over time energy flow $P_{\rm TE}$ is

$$P_{\rm TE} = \frac{\omega k_z}{32\pi\varkappa^2} ab(1+\delta_{n_1,0})(1+\delta_{n_2,0}), \tag{28}$$

with $N_{\rm TE} = 4P_{\rm TE}$. In the last expression, δ denotes the Kronecker symbol. Using notation $a_{\rm TE}$ for a_n of TE modes, from Eq. (6) and the current (19) we obtain (note that $\Delta j_{\omega,z}$ does

not contribute to $a_{\rm TE}$ because TE modes do not have E_z component of the electric field)

$$a_{\rm TE} = -\frac{1}{N_{\rm TE}} \int_0^{L_w} dz \int dx dy \Delta j_{\omega,x} E_x^- = -\frac{1}{N_{\rm TE}} \int_0^{L_w} dz e^{ikz} x_0'(z) E_x^-(0,0). \tag{29}$$

Similar to Eq. (24) one finds

$$|a_{\rm TE}|^2 P_{\rm TE} = \frac{8\pi q^2 \theta_0^2 k_w^2}{\omega a b} \frac{k^2 k_y^2}{k_z \varkappa^2 (1+\delta_{0,n_1})} \frac{\sin^2[\pi N_u (k-k_z)/k_w]}{[(k-k_z)^2 - k_w^2]^2} \times \cos^2 \frac{\pi n_1}{2} \sin^2 \frac{\pi n_2}{2}. \tag{30}$$

Using Eqs. (3) and (9) we obtain our final result for $\mathrm{Re}\, Z$

$$\mathrm{Re}\, Z(k) = 4 Z_0 \theta_0^2 F(k), \tag{31}$$

where the dimensionless function $F(k)$ is

$$F(k) = \frac{k_w^2}{abk} \sum_{n_1,n_2} \frac{1}{k_z} \left(\frac{k^2 k_y^2}{\varkappa^2 (1+\delta_{0,n_1})} + k_x^2 \left(\frac{k_z}{\varkappa} - \frac{\varkappa}{k-k_z} \right)^2 \right) \times \frac{\sin^2[\pi N_u (k-k_z)/k_w]}{[(k-k_z)^2 - k_w^2]^2}. \tag{32}$$

The summation in (32) goes over even values of n_1 (starting from $n_1 = 0$) and the odd values of n_2.

Let us consider the case of large N_u. In this case the last factor in (32) becomes highly peaked near the values of k which satisfy the equation

$$k - k_z(n_1, n_2) - k_w = 0, \tag{33}$$

where we have explicitly indicated that k_z depends on the integers n_1 and n_2 to emphasize that there may be many peaks corresponding to different values of these integers. These narrow peaks are due to the synchronism between the particle motion and one of the modes of the rectangular waveguide. When the condition of synchronism is satisfied, the particle resonantly radiate into the mode, which results in the increased value of the $\mathrm{Re}\, Z$ proportional to N_u^2. In the limit $N_u \to \infty$ the peaks in (32) become delta functions:

$$\frac{\sin^2[\pi N_u (k-k_z)/k_w]}{[(k-k_z)^2 - k_w^2]^2} \to \frac{\pi^2}{4k_w^3} N_u \delta\left(k - k_z - k_w\right). \tag{34}$$

We show in Appendix A that in the limit of large transverse cross-section of the pipe, $a, b \to \infty$, and a large number of periods, $N_u \to \infty$, Eq. (31) can be further simplified with the result in agreement with Eq. (2).

V. NUMERICAL CALCULATION OF CUR IMPEDANCE

To numerically calculate CUR, we used a computer code originally written for calculation of the coherent synchrotron radiation in a toroidal vacuum chamber with variable bending radius $R(s)$ [8]. The code solves the parabolic equation in the frequency domain in a curvilinear coordinate system with the origin on the beam trajectory [9–11]

$$\frac{\partial \boldsymbol{E}_\perp}{\partial s} = \frac{i}{2k}\left(\nabla_\perp^2 \boldsymbol{E}_\perp + \frac{2k^2 x}{R(s)}\boldsymbol{E}_\perp - 4\pi\nabla_\perp \rho_0\right), \tag{35}$$

where $\boldsymbol{E}_\perp$ is the transverse electric field, ρ_0 is the charge density, and $R(s)$ is the s-dependent bending radius. The longitudinal electric field is expressed in the terms of the transverse one,

$$E_s = \frac{i}{k}\left(\nabla_\perp \cdot \boldsymbol{E}_\perp - 4\pi\rho\right). \tag{36}$$

Eq. (35) is solved subject to the boundary conditions on the perfectly conducting walls [9, 12]

$$\boldsymbol{n} \times \boldsymbol{E}_\perp|_s = 0, \qquad E_s|_s = 0, \tag{37}$$

where $\boldsymbol{n}$ is the unit vector normal to the wall surface. In the code Eq. (35) is discretized on a rectangular two-dimensional mesh in x-y plane. To suppress numerical noise, we use a staggered grid scheme for the electric field [9] and ghost points outside of the boundaries.

Note that for a point charge the last term on the right hand side of Eq. (35) is singular. To avoid this singularity in numerical solution we treat the beam as having a small transverse size with rms values σ_x and σ_y in horizontal and vertical directions, respectively. In practical calculations, the typical values of σ_x and σ_y are set to be 0.1 mm and 0.01 mm.

It is assumed that the beam enters a curvilinear trajectory from a long straight pipe. The initial boundary condition for the equation (35) are given by the steady-state Coulomb field of the relativistic beam established in that straight waveguide [13].

The current version of the code deals with a rectangular cross section of the vacuum pipe with given transverse dimension a (along x) and b (along y). It is assumed that the shape of the cross-section (in the curvilinear coordinate system) does not change along s, and also that the beam position in x–y plane does not vary with s.

The inverse bending radius $R(s)$ for the undulator orbit is equal to the second derivative of $x_0(z)$, and for the orbit (13) is

$$\frac{1}{R(s)} = \theta_0 k_w \cos(k_w s). \tag{38}$$

Note that with this bending radius and our assumption that the shape of the pipe cross-section in the curvilinear coordinate system does not change with s, the simulated vacuum pipe wiggles together with beam orbit, as shown in Fig. 1. More precisely, while the horizontal walls of the pipe remain flat and parallel, the vertical ones follow the shape of the orbit in the undulator. This setup is somewhat different from the theoretical model developed in section IV, and we do not expect perfect agreement between the theory and the simulations.

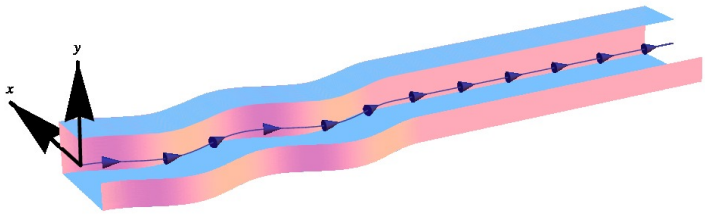

FIG. 1: The beam pipe in the undulator in numerical simulation. The wiggling pipe is followed by a straight waveguide of infinite length.

The longitudinal impedance is obtained by integration of E_s through the toroidal section. There is also a contribution to the impedance from the long straight exit pipe—we use a mode expansion method discussed in Refs. [9, 10] to calculate this contribution and to add it to the impedance of the undulator segment.

VI. AN EXAMPLE AND COMPARISON OF THE THEORY AND SIMULATIONS

As a first example, we calculated the CUR impedance of a wiggler with parameters similar to those of a section of the KEKB wiggler in the low energy ring [14]. The parameters of the wiggler are: wiggler period $\lambda_w = 1.087$ m, $\theta_0 = 1.1 \times 10^{-2}$ (this angle θ_0 corresponds to the undulator parameter $K = 76.57$ and the relativistic factor for the beam $\gamma = 6850$), $N_u = 10$. We assumed a square cross section for the beam pipe with the side equal to 94mm. The real part of the impedance calculated using the theory of Section IV and the the numerical code is shown in Fig. 2. In the figure one can clearly see sharp peaks in the region $k < 2$ mm^{-1}, which become less pronounce with increasing k.

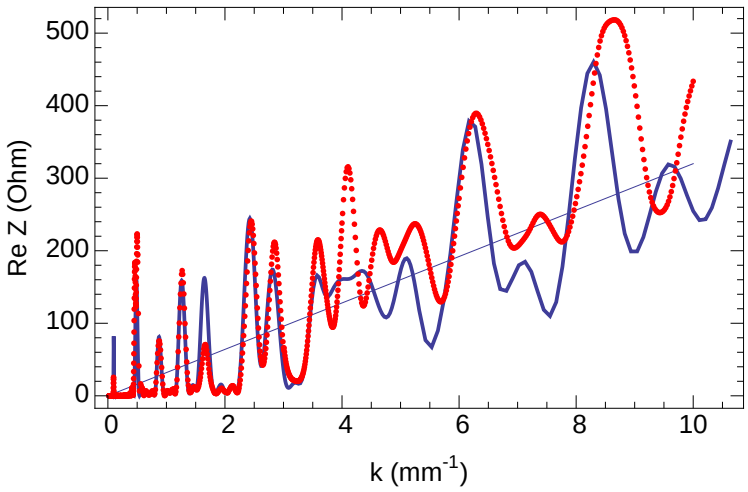

FIG. 2: Re Z as a function of the wavenumber k. The thick blue line is the theory, and the red dots are the simulation result. The thin straight line shows the free space impedance (2).

As is seen from Fig. 2, there is a noticeable disagreement between the theory and the simulations. As was pointed out above, the simulation assume a "wiggling pipe" in contrast to the straight waveguide in the theory. To verify that this is indeed the source of discrepancy, we calculated the same wiggler as above, but rectangular cross-section of the beam pipe was chosen to have a horizontal dimension of 100 mm and the vertical one of 20 mm. Increasing the horizontal size place the "wiggling walls" further away from the beam and suppresses their influence on the impedance. The result of the simulation is shown in Fig. 3 and demonstrate a very good agreement with the theory.

VII. SUPERKEKB WIGGLER

In our second example we used the magnetic field of the wiggler for the low energy SuperKEKB ring to compute particle's orbit. This field is composed from sections of dipole magnets with opposite polarity of the magnetic field interspersed with drift sections [15]. We assumed a square cross section of the pipe with the size of 90 mm. Fig. 4 shows the plot of the derivative dx_0/dz for the orbit inside the wiggler computed based on the magnetic field of the wiggler. One can see that the wiggler consists of 15 identical segments. The maximal angle dx_0/dz is of the order of 10^{-2}.

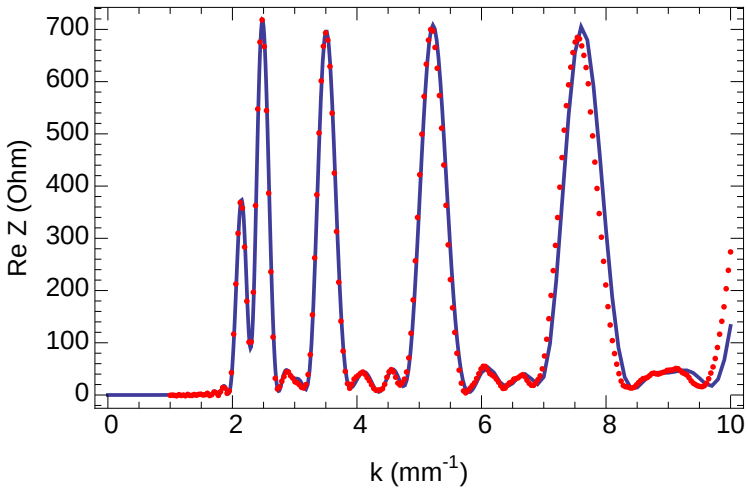

FIG. 3: Re Z as a function of the wavenumber k for a rectangular cross-section of the beam pipe with the aspect ratio 5. The thick blue line is the theory, and the red dots are the simulation result.

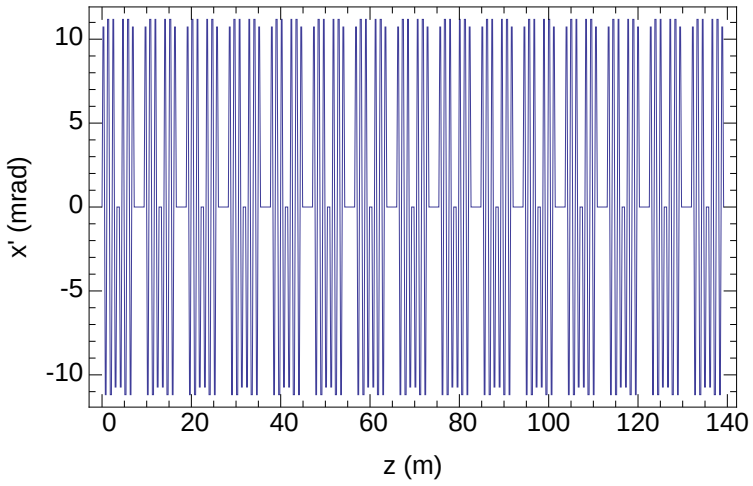

FIG. 4: The derivative dx_0/dz for particle's orbit in the wiggler.

As Fig. 4 shows, the orbit in the wiggler is different from a pure sinusoidal one assumed in (13). To understand the role of spectral harmonics in the orbit, we show in Fig. 5 a fraction of the spectrum of the function dx_0/dz. The dominant peaks in this spectrum correspond to the values $k \approx 5.34$ and $k \approx 6$ m^{-1}.

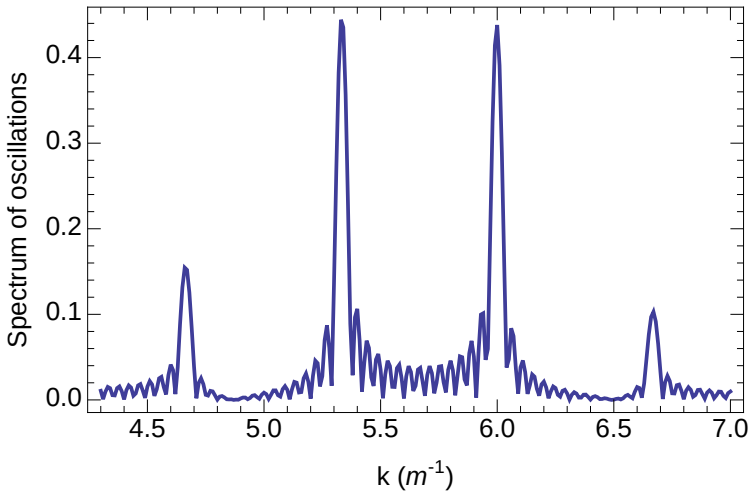

FIG. 5: Spectrum of the function shown in Fig. 4.

Using the computed orbit in the wiggler with the help of Eqs. (24) and (29) we computed numerically the amplitudes of the radiated waves, radiated power (9) and the real part of the impedance (3) which is shown in Fig. 6. One can see that again, the impedance demonstrates

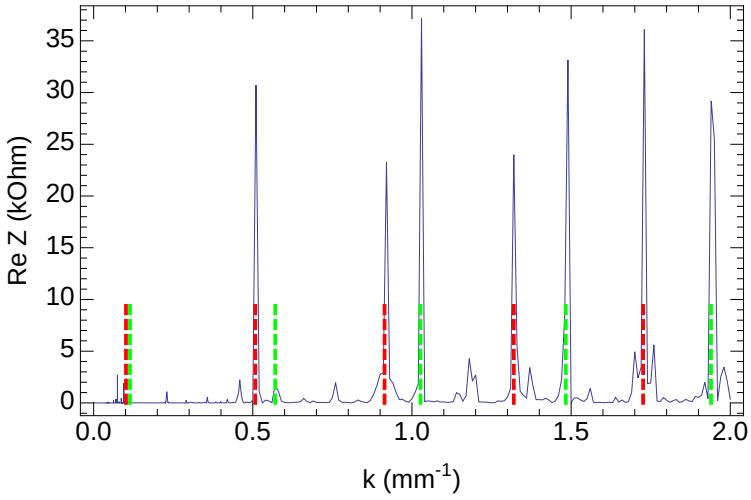

FIG. 6: Re Z as a function of the wavenumber k for the low energy SuperKEKB wiggler.

high and narrow peaks located at the synchronous frequencies (33). To identify the modes, we used Eq. (33) with two values of k_w corresponding to the highest peaks in Fig. 5. The

theoretically computed position of the beam are indicated by vertical dashed lines in Fig. 5 of different colors: red - $k_w \approx 6$ m^{-1} and green - $k_w \approx 5.34$ m^{-1} ($n_1, n_2 < 4$).

VIII. ACKNOWLEDGMENTS

We would like to thank K. Oide for useful discussions and providing the data for the SuperKEKB wiggler. The author DZ would also like to thank T. Agoh, K. Yokoya and K. Ohmi for helpful discussions during the CSR code's development. This work was done during stay of one of the authors (GS) at KEK, and he would like to thank his host K. Ohmi and the accelerator theory group for hospitality and support during this work. GS work was supported by the program of Short-term Visiting Scientist of High Energy Accelerator Research organization (KEK) and the U.S. Department of Energy under Contract No. DE-AC02-76SF00515.

[1] E. L. Saldin, E. A. Schneidmiller, and M. V. Yurkov, Nuclear Instruments and Methods, Sec. A, **417**, 158 (1998).

[2] J. Wu, T. Raubenheimer, and G. Stupakov, Phys. Rev. ST Accel. Beams, **6**, 040701 (2003).

[3] J. Wu, T. O. Raubenheimer, G. V. Stupakov, and Z. Huang, Phys. Rev. ST Accel. Beams, **6**, 104404 (2003).

[4] Y. H. Chin, *Coherent Radiation in Undulator*, Report LBL-29981 (LBL, 1990).

[5] A. W. Chao, *Physics of Collective Beam Instabilities in High Energy Accelerators* (Wiley, New York, 1993).

[6] L. A. Vainshtein, *Electromagnetic Waves* (Radio i svyaz', Moscow, 1988) in Russian.

[7] L. D. Landau and E. M. Lifshitz, *Electrodynamics of Continuous Media*, 2nd ed., Course of Theoretical Physics, Vol. 8 (Pergamon, London, 1960) (Translated from the Russian).

[8] D. Zhou, *Calculation of coherent synchrotron radiation impedance for a beam moving in a curved trajectory*, to be published.

[9] T. Agoh, *Dynamics of Coherent Synchrotron Radiation by Paraxial Approximation*, Ph.D. thesis, Department of Physics, University of Tokyo (2004).

[10] G. Stupakov and I. A. Kotelnikov, Phys. Rev. ST Accel. Beams, **12**, 104401 (2009).

[11] K. Oide, presentation at KEKB ARC 2009; K. Oide, in proceedings of PAC09.

[12] D. Gillingham and J. T.M. Antonsen, Phys. Rev. ST Accel. Beams, **10**, 054402 (2007).

[13] R. Alves-Pires, Tech. Rep. DPS/87-66 (CERN).

[14] K. Egawa et al., Nuclear Instruments and Methods, Sec. A, **499**, 24 (2003).

[15] K. Oide, private communication.

APPENDIX A: LIMIT IF $N_u \to \infty$

In the limit $N_u \to \infty$ we use (34) and find for the function F

$$F(k) = \frac{k_w^2}{abk} \sum_{n_1,n_2} \left(\frac{k^2 {k_y}^2}{k_z \varkappa^2 (1+\delta_{0,n_1})} + \frac{k_x^2 \varkappa^2}{k_z} \left(\frac{k_z}{\varkappa^2} - \frac{1}{k-k_z} \right)^2 \right) \times \frac{\pi^2}{4k_w^3} N_u \delta\left(k - k_z - k_w\right). \tag{A1}$$

Taking into account that in this limit the main contribution to the sum is due to many modes with $n_1 \gg 1$ and $n_2 \gg 1$ we also replace summation by integration

$$\sum_{n_1,n_2} \to \frac{1}{4} \int_0^\infty dn_1 \int_0^\infty dn_2 = \frac{ab}{4\pi^2} \int_0^\infty dk_x \int_0^\infty dk_y \tag{A2}$$

and drop the term δ_{0,n_1}. Note that for $k \gg k_w$ the argument of the delta-function becomes equal to zero for small values of $k_x \sim k_y \sim \sqrt{k k_w} \ll k$, so that

$$k - k_z - k_w = k - \sqrt{k^2 - \varkappa^2} - k_w \approx \frac{1}{2k} \varkappa^2 - k_w. \tag{A3}$$

We can now replace $k - k_z$ by $\varkappa^2/2k$ and k_z by k in (A1) to obtain

$$F(k) = \frac{N_u k}{8 k_w} \int_0^\infty dk_x \int_0^\infty dk_y \delta\left(\varkappa^2 - 2k k_w\right) = \frac{\pi N_u k}{32 k_w}, \tag{A4}$$

which gives for the real part of the impedance (see (31))

$$\mathrm{Re}\, Z = \frac{1}{16} Z_0 L_w k \theta_0^2 \tag{A5}$$

in agreement with (2).